Biochimica et Biophysica Acta, 647 (1981) 7–17
Elsevier/North-Holland Biomedical Press

BBA 79364

THE EFFECT OF CYTOCHROME OXIDASE ON LIPID CHAIN DYNAMICS

A NANOSECOND FLUORESCENCE DEPOLARIZATION STUDY

KAZUHIKO KINOSITA, Jr. [a], SUGURU KAWATO [a,*], AKIRA IKEGAMI [a], SATOSHI YOSHIDA [b,**] and YUTAKA ORII [c]

[a] *Institute of Physical and Chemical Research, Hirosawa, Wako-shi, Saitama 351,* [b] *Department of Biophysical Engineering, Faculty of Engineering Science, Osaka University, Toyonaka, Osaka 560 and* [c] *Department of Public Health, Faculty of Medicine, Kyoto University, Kyoto 606 (Japan)*

(Received February 24th, 1981)

Key words: Fluorescence depolarization; Cytochrome oxidase; Boundary lipid; Diphenyl hexatriene; Wobbling motion; Lipid chain dynamics

Molecular motions in membranes composed of purified cytochrome oxidase (EC 1.9.3.1) and synthetic lipid (L-α-dimyristoylphosphatidylcholine or L-α-dioleoylphosphatidylcholine) at various ratios were investigated with a lipophilic fluorescent probe 1,6-diphenyl-1,3,5-hexatriene. Nanosecond fluorescence depolarization kinetics of the probe showed that the rod-shaped probe molecules perform a fast wobbling motion (restricted rotation) in all membranes studied, presumably reflecting the motion of lipid acyl chains. At temperatures where the pure lipid was in the liquid-crystalline phase, presence of cytochrome oxidase reduced the angular range of the wobbling motion, whereas its rate; the wobbling diffusion constant, was unaffected. On the other hand, incorporation of the protein into lipid in the gel phase resulted in the increase in the wobbling diffusion constant while the range of the wobbling motion remained the same. A time-dependent view of lipid dynamics that accounts for the above findings, as well as the results of recent electron spin resonance and nuclear spin resonance studies of protein-lipid interactions, is proposed.

Introduction

Nanosecond (time-resolved) fluorescence depolarization measurement can provide useful information about the dynamic structure of supramolecular systems. Both the rate of rotation (wobbling diffusion constant) and the degree of orientational constraint of constituent molecules can be estimated from a single measurement [1]. Investigations using the lipophilic fluorescent probe 1,6-diphenyl-1,3,5-hexatriene (DPH) have been performed to determine the nature of the thermotropic phase transition in lipid bilayers [2–5], the effect of cholesterol on the dynamics of lipid hydrocarbon chains [5–7], and the dynamic structure of various biological membranes [8,9].

Here we report a study of lipid-protein interaction in a simple system composed of purified cytochrome oxidase (EC 1.9.3.1) and synthetic lipid. Electron spin resonance (ESR) studies have shown that membrane proteins, such as cytochrome oxidase, are sur-

* Present address: Laboratorium für Biochemie, Eidgenössische Technische Hochschule Zürich, CH-8092 Zürich, Switzerland.

** Present address: Department of Chemistry and Laboratory of Bioenergetics, State University of New York at Albany, Albany, NY 12 222, U.S.A.

Abbreviations: DMPC, L-α-dimyristoylphosphatidylcholine; DOPC, L-α-dioleoylphosphatidylcholine; DPH, 1,6-diphenyl-1,3,5-hexatriene; buffer A, 50 mM sodium phosphate buffer (pH 7.4) containing 0.25% (v/v) Emasol 1130 and 0.1% (w/v) sodium cholate; ESR, electron spin resonance; NMR, nuclear magnetic resonance.

rounded by a layer of immobilized lipid, termed either 'boundary lipid' [10–12] or 'annular lipid' [13,14]. A deuterium nuclear magnetic resonance (^{2}H-NMR) study [15] also supported this view, but subsequent NMR studies [16–19] failed to detect the immobilized lipid and even showed that proteins disorder the lipid hydrocarbon chains. The apparent discrepancy between the ESR and NMR results has been ascribed to the difference in the time window of the two techniques. Our fluorescence study with a time window of nanoseconds, which is not much different from that of conventional ESR, also showed restriction of molecular motions in the presence of cytochrome oxidase, but at the same time suggested a high rate of lipid chain wobbling on the surface of the protein. The distinction between the angular amplitude and the rate of wobbling motion helps construct a unified view of the effect of membrane protein on neighboring lipid chains.

This work is part of a series of investigations on cytochrome oxidase in reconstituted systems. Previous studies [20–22] mainly focused on protein part, where the oxidase has been shown to undergo two types of temperature-induced conformational changes, one intrinsic to cytochrome oxidase and the other induced by the lipid phase transition. The present study sheds some light on the nature of interaction between cytochrome oxidase and surrounding lipid.

Experimental Procedures

Materials. Cytochrome oxidase was prepared from bovine heart muscle by the method of Okunuki et al. [23] with some modifications. The final ammonium sulfate precipitate was dissolved in 50 mM sodium phosphate buffer (pH 7.4) containing 0.25% (v/v) Emasol 1 130 and 0.1% (w/v) sodium cholate (buffer A), and dialysed against sufficient volume of the buffer A in the cold. The dialysate was kept frozen in liquid nitrogen and was thawed immediately before use. Two different batches of oxidase were used in this study with A_{280nm}/A_{420nm} (oxidized) of 2.51 and 2.64, respectively (10.5–10.2 nmol heme *a*/mg protein). Specific activities of these enzyme preparations were 10.0 and 9.0 s^{-1} per mg protein per 3 ml of reaction mixture, respectively, when assayed spectrophotometrically by following the rate of oxidation of ferrocytochrome *c* at 550 nm [24]; the assay medium contained 15 μM of reduced cytochrome *c* in 15 mM NaCl plus 75 mM sodium phosphate buffer, pH 6.0. The concentration of oxidase was determined from millimolar extinction coefficient difference of 16.5 ($\Delta\epsilon$ (605 nm-630 nm), reduced). The molar concentration of the oxidase in this paper refers to that of heme *a*.

L-α-Dimyristoylphosphatidylcholine (DMPC) and L-α-dioleoylphosphatidylcholine (DOPC) were purchased from Sigma and used without further purification. DPH was obtained from Aldrich. Cytochrome *c* (Horse heart, Sigma Type VI) was reduced with dithionite and residual dithionite was removed with a Sephadex G-25 column. Cholate was recrystallized from ethanol/water. Other chemicals were of reagent grade.

Preparation of cytochrome oxidase vesicles. Lipid vesicles containing cytochrome oxidase were prepared essentially according to Yoshida et al. [20]. In a typical preparation, 0.75 mg of lipid in chloroform was dried onto the wall of a test tube under high vacuum. Approx. 250 μl (exact amount was so chosen that the final volume of the dialysate became 300 μl) of 50 mM sodium phosphate buffer (pH 7.4) containing 2 mM $MgSO_4$ and 15 μl of 20% (w/v) sodium cholate were added to the test tube, and the mixture was vortexed at 40–50°C until it became clear. The solution was cooled to 0°C and cytochrome oxidase in buffer A (700 to 1 000 μM) was added to give a desired protein/lipid ratio. In order to ensure complete mixing, the final mixture of 300 μl was sonicated for 10 min in an ice bath with a bath-type sonicator (Choonpa Kogyo, Model USV-150V) operated at 50 kHz at 150 W. The solution was then dialysed for 20 h at 4°C against four changes, 500 ml each, of the phosphate buffer containing $MgSO_4$. Vesicle suspension obtained by the dialysis was diluted with the same buffer to a total volume of 3.0 ml and kept at 4°C; all experiments were done within two days after preparation. Vesicles prepared by the above method had variable sizes, but sucrose density gradient centrifugation gave a single narrow band whose position depended on the protein/lipid ratio [20]. Residual cholate level under similar dialysis procedure has been reported to be less than 30 μg of cholate/mg protein [12]; Rice et al. [19] have reported a level of about 3 wt%, with respect to total

membrane mass, under slightly different conditions.

Incorporation of DPH. 2 to 4 μl of DPH solution in tetrahydrofuran was added to 3 ml of the oxidase-lipid suspension so that the molar ratio of DPH to lipid became 1/500. The suspension was then incubated at 30°C for 2 h with occasional mixing. The samples were protected from light during the incubation and immediately subjected to fluorescence measurement. For steady-state fluorescence measurements, the lipid concentration in the sample was chosen to be 14 μM, since plots of fluorescence anisotropy vs. concentration revealed that depolarization due to light scattering was practically negligible at this concentration even with the highest oxidase to lipid ratio. Lipid concentration in samples for the nanosecond measurement was 70 to 140 μM; the nanosecond data were therefore corrected for the effect of light scattering as described below.

Fluorescence measurement. Nanosecond time-resolved fluorescence depolarization was measured by the nanosecond fluorometer as previously described [25]. The performance of the fluorometer has been greatly improved by the adoption of a newly developed light pulser and a Hamamatsu TV R943-02 photomultiplier tube (to be described elsewhere). The pulser produced intense light pulses of duration less than 0.8 ns (full width at half maximum) at a frequency around 10 kHz. Light at 360 nm was selected by combination of a monochromator and Hoya U-340 filters, polarized vertically by a Glan prism, and focused onto the sample placed in a thermostatted cell holder. Fluorescence emitted at 90° to the exciting beam was collected through Hoya L-39 and L-42 filters (transmission above 420 nm). A sheet polarizer (Polaroid HNP'B) sequentially analyzed the fluorescence into vertically and horizontally polarized components, $I_V(t)$ and $I_H(t)$, which were recorded by the single photon counting technique. The apparatus response function, $g(t)$, was measured at 455 nm with a dilute Ludox (Du Pont) suspension in place of the sample [3]. Since samples containing oxidase gave weak, short-lived fluorescence in the absence of DPH, the blank fluorescence was measured under identical conditions and subtracted from the corresponding data. In no cases was the peak value of the blank fluorescence more than 5% of that of DPH fluorescence.

Steady-state fluorescence intensities, I_V^S and I_H^S, were measured by the same fluorometer operated as an ordinary photon counter. Excitation light from a 500-W xenon lamp was attenuated with Zeiss neutral density filters; bleaching of DPH [26] was not observed at the low light level. In temperature scan experiments, the sample was heated at a rate of 15°C/h and the temperature was monitored with a tip thermister immersed in the sample. Fluorescence anisotropy always returned to the original value upon cooling.

Analysis of fluorescence data. From the observed intensites I_V and I_H, total fluorescence intensity I_T, difference intensity I_D, and fluorescence anisotropy r were calculated as follows:

$$I_T = I_V + 2SI_H \tag{1}$$

$$I_D = (I_V - SI_H)/D \tag{2}$$

$$r = I_D/I_T \tag{3}$$

where S is the ratio of the sensitivities of the detection system for vertically and horizontally polarized light and was taken equal to I_V/I_H obtained with horizontally polarized excitation. The denominator D in Eqn. 2 represents the extent of depolarization due to the scattering of excitation light and emitted fluorescence, and was taken as 1 for steady-state data. For time-dependent data, which were obtained at higher vesicle concentrations, D was so chosen as to satisfy the following equation:

$$\int I_D(t)\mathrm{d}t / \int I_T(t)\mathrm{d}t = r^S \tag{4}$$

where r^S is the corresponding steady-state anisotropy *.

---

* If we put a superscript 0 to quantities that would be obtained in the absence of light scattering, we can show from symmetry considerations that

$I_V = (1 - \delta)I_V^0 + \delta I_H^0$ and $I_H = (1 - \delta')I_H^0 + \delta' I_V^0$

where δ and δ' are constants that depend only on the extent of scattering. Then,

$I_D = I_V - I_H = (1 - \delta - \delta')I_D^0$ and

$I_T = I_V + 2I_H = I_T^0 + (2\delta' - \delta)(I_V^0 - I_H^0)$

For small δ and δ', i.e. if the scattering is not very severe, we can show that $\delta \simeq 2\delta'$. Thus, light scattering reduces I_D (and therefore r) by a constant factor that is practically independent of the value of r. The factor D in Eqn. 2 in the text corresponds to $1 - \delta - \delta'$. Note that here we are not concerned with the scattered excitation light that reaches the photocathode, which can usually be eliminated by suitable combination of filters.

The nanosecond decay data were analyzed by assuming exponential decays of the following forms:

$$I_T^{\delta}(t) = C[\alpha_1 \exp(-t/\tau_1) + \alpha_2 \exp(-t/\tau_2)] \quad (5)$$

$$r^{\delta}(t) = (r_0 - r_\infty) \exp(-t/\varphi) + r_\infty \quad (6)$$

where the superscript δ indicates that these quantities are responses to truely impulsive (δ-function like) excitation, and C is a constant that ensures $\alpha_1 + \alpha_2 = 1$. The parameters α_i, τ_i, r_∞, and φ were so determined that the convoluted products

$$I_T^{calcd}(t) \equiv \int g(t') I_T^{\delta}(t - t') dt' \quad (7)$$

$$I_D^{calcd}(t) \equiv \int g(t') r^{\delta}(t - t') I_T^{\delta}(t - t') dt' \quad (8)$$

best fitted the observed $I_T(t)$ and $I_D(t)$, respectively [3,25]. The limiting anisotropy, r_0, of DPH was taken as 0.395 [3]. All calculations were done by a FACOM 230-75 computer. Note that the above procedure assigns the same $r^{\delta}(t)$ to all of the DPH population in the sample; r_∞ and φ obtained should therefore be considered as averaged quantities (see below).

Results

Steady-state anisotropy

Fig. 1 shows the steady-state fluorescence anisotropy, r^s, of DPH in oxidase-DMPC vesicles. In pure DMPC vesicles, r^s decreased sharply at about 23°C, reflecting the gel to liquid-crystalline phase transition in DMPC bilayers [27]. Below the phase transition, addition of cytochrome oxidase had little effect on r^s. In the liquid-crystalline phase, on the other hand, presence of the membrane protein greatly increased r^s, the effect being basically proportional to the oxidase/lipid ratio in the range examined. The phase transition was no longer observed at the molar ratio of 4/100. A very similar temperature profile has been reported for bacteriorhodopsin-DMPC membranes [28].

In pure DOPC vesicles, for which the transition temperature is about −22°C [27], r^s of DPH decreased regularly from 0.16 at 4°C to 0.06 at 40°C (data not shown). When DOPC vesicles contained cytochrome oxidase at a molar ratio of 2/100, r^s was higher by about 0.09 at all temperatures between 4 and 40°C. Thus the effect of oxidase on DOPC vesicles is similar to that on DMPC in the liquid-crystalline phase.

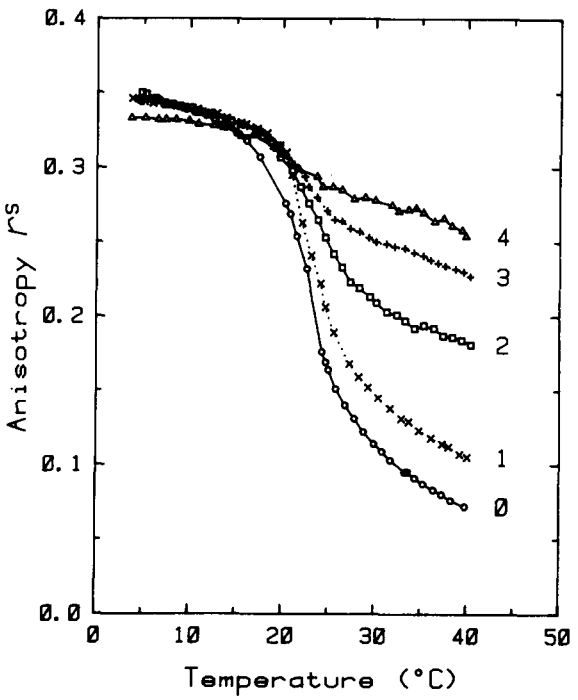

Fig. 1. Steady-state fluorescence anisotropy, r^s, of DPH in oxidase-DMPC vesicles against temperature. Vesicles were prepared by cholate dialysis and suspended in 50 mM sodium phosphate buffer containing 2 mM $MgSO_4$ as described in text. The sample contained 0.028 μM of DPH and 14 μM of DMPC. The numbers at the end of each curve show the number of cytochrome oxidase molecules (based on heme *a*) per 100 DMPC molecules. Heating scan at a rate of 15°C/h. Reproducibility of r^s values from preparation to preparation was within 0.01 at 10°C and 0.02 at 35°C.

Nanosecond depolarization kinetics and the wobbling motion of DPH

The steady-state data suggested differential effects of cytochrome oxidase on lipid chain motions depending on whether the lipid was in the gel or in the liquid-crystalline phase. The nanosecond fluorescence depolarization measurements were therefore performed at 10 and 35°C, below and above the transition temperature of DMPC. As seen in Fig. 2, decay of fluorescence anisotropy, $r(t)$, after the pulsed excitation was always biphasic, consisting of a rapid initial decrease followed by an almost constant

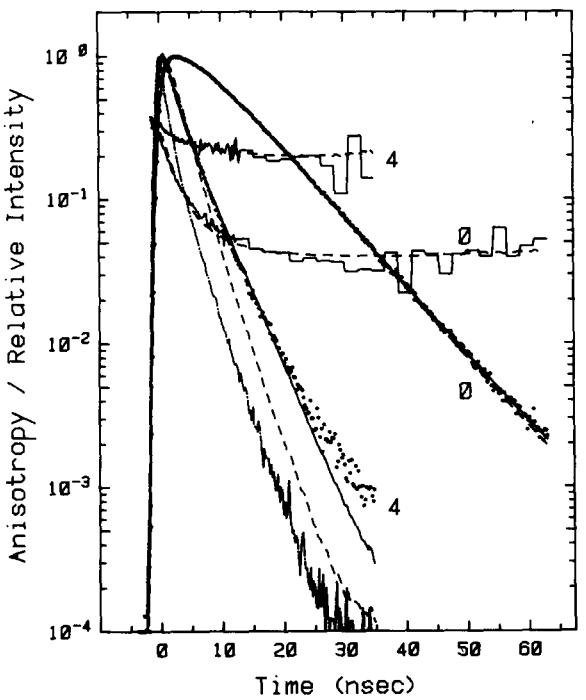

Fig. 2. Fluorescence decay of DPH in pure DMPC vesicles (curves 0) and in vesicles of the oxidase-to-DMPC molar ratio of 4/100 (curves 4). Chain line, the instrumental response function, $g(t)$; dots, the total fluorescence intensity, $I_T(t)$; zigzag solid curves, fluorescence anisotropy, $r(t)$. The broken and solid lines superimposed on $I_T(t)$ are the calculated best fit curves for single and double exponential approximations, respectively. The broken lines on $r(t)$ are the best fit curves for the constant-plus-exponential approximation (Eqn. 6 in text). DMPC concentration was 70 μM for curves 0 and 140 μM for curves 4. Molar ratio of DPH to DMPC was 1/500.

phase. Similar biphasic decay of DPH anisotropy has been observed in many membrane systems [2–4, 6–9]. Presence of the finite asymptote, r_∞, indicates that the orientation of the rod-shaped DPH molecule is restricted in the membranes, whereas the rapidly decreasing phase detects the rotational Brownian motion of DPH within the allowed orientations.

For quantitative description of the restricted rotation, we analyzed the anisotropy decay in terms of the wobbling-in-cone model [1,3] where the long axis of DPH wobbles freely in a cone of half angle θ_c with a wobbling diffusion constant D_w. The model, to a good approximation, predicts an anisotropy decay of the form represented by Eqn. 6. The broken lines superimposed on the zigzag anisotropy decays in Fig. 2 show the calculated best fit curves based on Eqn. 6 (i.e. Eqn. 8 divided by Eqn. 7) and indicate that the model in fact can approximate the observed data. The values of r_∞ and φ that gave the best fit for each data are listed in Table I. From these values, the cone angle θ_c and the wobbling diffusion constant D_w were calculated as previously described [1] *. The results are shown in Fig. 3. As will be discussed below, some of DPH in the present system is quenched by oxidase and their motions are not reflected in these parameters.

The wobbling motion of DPH in pure DMPC vesicles was very close to that in dipalmitoylphosphatidylcholine vesicles [3]. In the gel phase, the motion was relatively slow and restricted to a cone angle of approx. 20°. The wobbling diffusion constant of 0.02 ns^{-1} corresponds to the 'viscosity in the cone' [3] of 1.9 P. This value represents the dynamic friction against the wobbling motion and should be distinguished from the 'microviscosity' [30] which mainly reflects the static orientational constraint. In the liquid-crystalline phase at 35°C, DPH wobbled as far as ±70° with D_w an order of magnitude larger than that at 10°C. the viscosity in the cone was approx. 0.3 P at 35°C.

The effect of oxidase on the wobbling motion of DPH was markedly different at the two temperatures investigated. Above the phase transition, addition of the protein progressively reduced θ_c while D_w remained the same. Table I indicates that the increase in r^s at high temperatures (Fig. 1) was due largely to the increase in r_∞, or equivalently, to the decrease in θ_c. Below the phase transition, on the other hand, presence of oxidase increased D_w toward the value in the liquid-crystalline phase whereas the already narrow cone angle was not affected. On the whole, the effect of cytochrome oxidase was to converge D_w to the value in pure lipid in the liquid-crystalline phase and θ_c to the value in the gel phase, irrespective of temperature. This result is qualitatively similar to the effect of cholesterol [7].

* Recent calculations [29] have shown that the wobbling-in-cone analysis is valid even if the orientational distribution of the DPH axis is of a Gaussian type instead of the square-well type. In the case of the Gaussian distribution, θ_c approximates to the effective angular width, defined as the angle beyond which the fractional population is $1/e^2$ = 0.135 of the total.

TABLE I

FLUORESCENCE ANISOTROPY DECAY PARAMETERS OF DPH IN OXIDASE/LIPID VESICLES

The residual anisotropy r_∞ and the apparent relaxation time φ are defined by Eqn. 6 in text. Each value is an average over two to four samples; numbers in parentheses indicate the standard deviation. In the curve-fitting procedure, the decay of total fluorescence intensity, $I_T(t)$, was approximated with two exponentials as in Eqn. 5 in text. Three-exponential approximation of $I_T(t)$ was also tried for the data at the oxidase/DMPC ratio of 4/100, yielding a closer fit between the experimental and calculated $I_T(t)$. Values of r_∞ and φ, however, remained within the range listed below.

Lipid	Oxidase/lipid molar ratio	10°C		35°C	
		r_∞	φ (ns)	r_∞	φ (ns)
DMPC	0/100	0.330 (0.001)	1.62 (0.04)	0.036 (0.004)	1.46 (0.07)
	1/100	0.345 (0.001)	0.48 (0.13)	0.052 (0.004)	1.41 (0.12)
	2/100	0.347 (0.010)	0.27 (0.04)	0.083 (0.021)	1.13 (0.22)
	3/100	0.335 (0.001)	0.24 (0.07)	0.161 (0.025)	0.85 (0.30)
	4/100	0.342 (0.016)	0.24 (0.08)	0.186 (0.002)	0.89 (0.06)
DOPC	0/100	0.024 (0.002)	4.06 (0.11)	0.004 (0.001)	1.33 (0.06)
	2/100	0.092 (0.003)	2.68 (0.09)	0.051 (0.006)	1.09 (0.10)

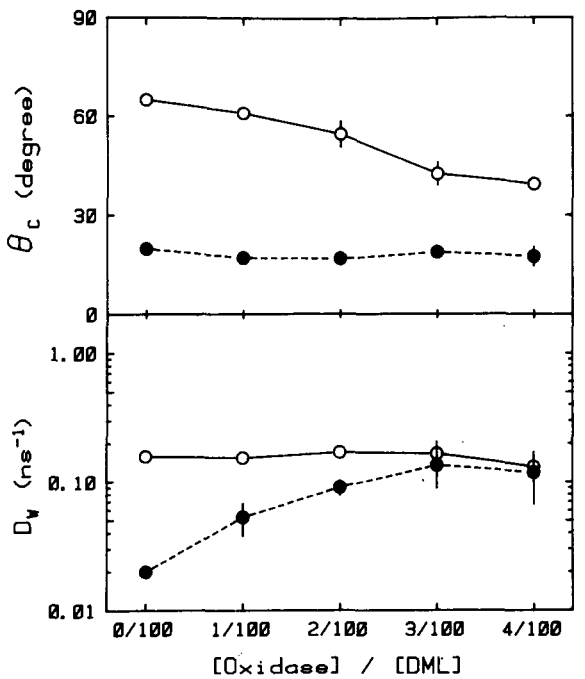

Fig. 3. The wobbling diffusion constant, D_W, and the cone angle, θ_c, for the wobbling motion of DPH in oxidase-DMPC vesicles. ○, at 35°C; ●, at 10°C. These parameters were determined from the fluorescence anisotropy decays as described in text. Each point is an average over two to four samples. The vertical bars represent standard deviation; where not indicated, the deviation was smaller than the size of the symbol. DML, DMPC.

As has been suggested by the steady-state anisotropy data, the effect of oxidase on DOPC was essentially the same as the effect on liquid-crystalline DMPC. The absence or the presence of oxidase at a molar ratio of 2/100 did not affect D_W within experimental error both at 10°C ($D_W = 0.06$ ns^{-1}) and at 35°C ($D_W = 0.19$ ns^{-1}). By contrast, θ_c was found smaller in oxidase-containing vesicles: θ_c in pure DOPC was 69° at 10°C and 80° at 35°C; these values were reduced to 53° and 61° in the presence of oxidase.

Fluorescence lifetime of DPH in oxidase-containing vesicles

Lifetime of DPH fluorescence was shorter in the presence of oxidase than in pure lipid vesicles, as seen in Fig. 2. Morever, the decay of total fluorescence intensity, $I_T(t)$, was clearly deviated from single exponential in vesicles containing oxidase. For technical simplicity, we analyzed $I_T(t)$ with the two-exponential approximation as in Eqn. 5. The results are summarized in Fig. 4. In pure DMPC vesicles, $I_T(t)$ decayed almost single-exponentially both below and above the phase transition. Cytochrome oxidase even at the molar ratio of 1/100 greatly reduced the average lifetime and caused marked deviation from a simple exponential decay.

Two mechanisms are conceivable for the observed

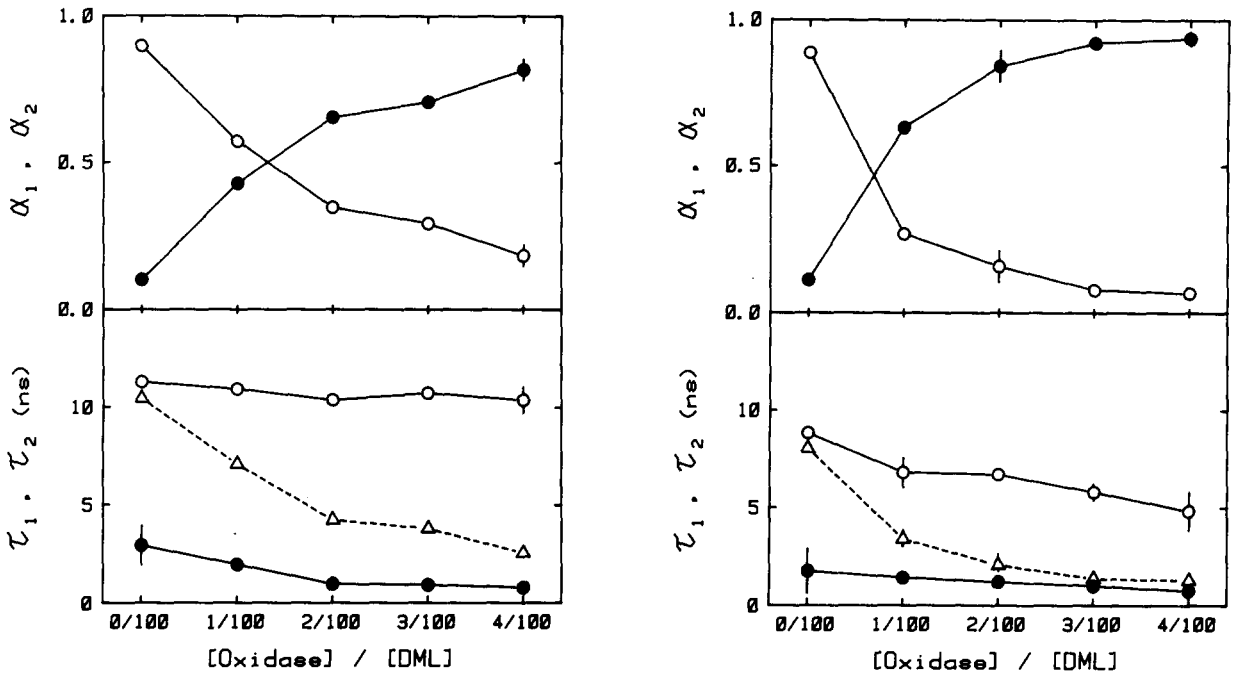

Fig. 4. Fluorescence intensity decay parameters for DPH in oxidase-DMPC vesicles at 10°C (left) and at 35°C (right). The total fluorescence intensity, $I_T(t)$, was analyzed in terms of double exponential approximation, $I_T^R(t) \propto \alpha_1 \exp(-t/\tau_1) + \alpha_2 \exp(-t/\tau_2)$. •, short-lived component; ○, long-lived component; Δ, average lifetime, $\langle\tau\rangle \equiv \alpha_1\tau_1 + \alpha_2\tau_2$. Each point is the average over two to four samples. The vertical bars represent standard deviation; where not indicated, the deviation was smaller than the size of the symbol. DML, DMPC.

quenching of DPH fluorescence. One is the excitation energy transfer from DPH to heme *a*, which must be efficient because the strong Soret absorption band of heme *a* overlaps with the emission spectrum of DPH. We estimate R_0, the distance for the energy transfer with 50% efficiency [31], to be 5.1 nm for random orientations. (The approximate 4-fold symmetry of the heme plane [32] and the rapid wobbling of DPH make R_0 relatively insensitive to the orientational factor.) The R_0 value is approximately the same as the dimension of the cytochrome oxidase complex in membrane [33,34]. Fluorescence of DPH in close vicinity to oxidase is therefore severely quenched. The energy transfer results in a distribution of fluorescence lifetimes. The two-exponential analysis (Fig. 4) is only an approximation to this continuous distribution.

The other possibility is that the microenvironment of DPH in lipid-poor vesicles is less hydrophobic than the interior of pure lipid bilayer; DPH might even be partially exposed to water. This latter mechanism, however, is not probably dominant in the present case as suggested by the following observation: addition of 0.5 M potassium iodide (prepared fresh), known to be an efficient quencher of DPH fluorescence [35], to vesicles of oxidase/DMPC ratio of 1/100 decreased average lifetime $\langle\tau\rangle \equiv \alpha_1\tau_1 + \alpha_2\tau_2$ from 7.1 ns to 6.2 ns at 10°C and from 3.0 ns to 2.5 ns at 35°C. For DPH dissolved in methanol, KI was much more effective: $\langle\tau\rangle$ was reduced from 6.2 ns to 3.1 ns at 10°C and from 3.2 ns to 1.9 ns at 35°C. Thus, most of fluorescent DPH in the membrane was not accessible to the iodide ions. At higher oxidase/DMPC ratios, KI was less effective mainly because $\langle\tau\rangle$ was already very short in the absence of KI.

Discussion

DPH as a probe for the dynamics of lipid acyl chains

DPH is not fluorescent in water but strongly fluo-

resces when incorporated in membranes [30]. It is a lipophilic molecule and enters in between lipid acyl chains whether they are in the gel phase or in the liquid-crystalline phase with equal affinity [36]. Because the thickness as well as the length of the rod-shaped DPH approximates to those of a lipid acyl chain (approx. 0.5 nm thick and 1.5–2 nm long), DPH presumably replaces one acyl chain in the membrane. Then the motion of DPH must closely reflect that of lipid acyl chains because DPH can wobble only when one of the neighboring chains wobbles out of its place.

The quenching of DPH fluorescence due to the energy transfer to heme *a* (Fig. 4) suggests that DPH also enters into and reports the dynamics of boundary lipid regions. From the critical distance for energy transfer, R_0, of 5.1 nm, we estimate that the fluorescence lifetime of DPH is about 0.1 ns for a DPH to heme *a* distance of 2.4 nm, 1 ns for 3.5 nm, and 4 ns for 5 nm. On the other hand, the size of the oxidase complex in the plane of membrane has been estimated to be about 5 nm × 6 nm [33]. Its precise shape, however, appears to be irregular and the largest dimension extends to about 10 nm; its vertical dimension is 11 nm, far exceeding the bilayer thickness of about 4 nm [34]. Though lack of information on the exact location of heme *a* in the protein precludes precise estimation, we expect that the lifetimes of DPH at the protein surface are distributed around 1 ns, ranging between zero to several nanoseconds. (Note that the vertical separation between DPH and heme *a*, which may well be a few nm, should be taken into account in the estimation of the lifetimes.) The decay of total fluorescence intensity in the sample of oxidase/lipid ratio of 4/100, where the amount of lipid is barely enough to surround the oxidase complex with a single layer of lipid acyl chains [10], is consistent with such distribution.

The analysis of anisotropy decay

In view of the probable heterogeneity in the motional properties of DPH in the membrane, especially at intermediate oxidase/lipid ratios, D_w and θ_c in Fig. 3 should be regarded as gross indices of average DPH dynamics. The average ignores those DPH with very short fluorescence lifetimes, i.e. those in the immediate vicinity to heme *a*, because contribution of the short-lived components to $r(t)$ decreases rapidly with time. Since the experimental parameters φ and r_∞, from which D_w and θ_c are calculated, mainly reflect the behavior of $r(t)$ at $t \gtrsim \varphi$, the results in Fig. 3 refer to those DPH with lifetimes τ not much less than φ. (The time dependence of $r(t)$ may partially depend on the lifetime distribution if there is a strong correlation between the lifetime and motional properties [37]. However, the relaxation time for the wobbling motion of those DPH with $\tau \gtrsim \varphi$ cannot be much different from φ.)

Fig. 3 shows that, in the presence of cytochrome oxidase, motion of DPH is severely restricted in angular range but the rate of wobbling remains high. As discussed above, this statement applies to those DPH with $\tau \gtrsim \varphi$. At 35°C, for example, φ was about 1 ns (Table I). The condition $\tau \gtrsim \varphi$ thus translates into $d \gtrsim 3.5$ nm, where d is the center-to-center distance between DPH and heme *a*. The geometry of oxidase suggests that significant amount of DPH at the protein surface will satisfy this condition. At the highest oxidase/lipid ratio of 4/100, in particular, virtually all DPH molecules are at or very close to the protein surface. (Three-exponential analysis of $I_T(t)$ at 35°C in fact showed that more than 99% of DPH in this sample satisfied $d < 8$ nm.) D_w and θ_c in this sample are therefore expected to reflect the DPH dynamics in the vicinity of the protein.

Not much information is available concerning the quenched ($\tau < \varphi$) DPH. However, the very irregular shape of the oxidase suggests that those DPH with $\tau \gtrsim \varphi$ in the highest oxidase/lipid membrane may be more or less randomly chosen samples of the 'boundary' DPH (the distance to heme *a* does not necessarily correlate with the distance to the protein surface). It is likely that the quenched DPH also wobbles rapidly in a narrow angular range.

Here it should be noted that the angular range reported by fluorescence refers to the motion in the nanosecond time range and does not necessarily deny the presence of large amplitude rotations in the micro- and millisecond time ranges as will be discussed below. Also, the axis of the wobbling motion does not necessarily coincide with the normal of the membrane. In the neighborhood of the protein, lipid chains as well as DPH probably lie along the irregular surface of the protein, as has been suggested by Jost et al. [10], and wobble in narrow pseudo-potential wells formed by the protein surface and the surround-

ing lipid molecules. The axis of the wobbling motion of DPH therefore may well be different from DPH to DPH. Such variations in the direction of wobbling axes are not detected in the present experiments, because the fluorescence depolarization results from the rotation of individual molecules.

Dynamics of boundary lipid

Using spin-labeled fatty acid, Jost et al. [10,11] have suggested the presence of immobilized lipid acyl chains in membranes containing cytochrome oxidase. The amount of the immobilized lipid was estimated to be about 50 molecules per oxidase complex containing two heme *a*'s. They proposed that these immobilized molecules constitute a single layer of 'boundary lipid' between the hydrophobic surface of the membrane protein and fluid lipid bilayer. Basically the same conclusion was reached with spin-labeled phospholipid [12], though Knowles et al. [38] have shown that the immobilizing effect of the protein extends, to some extent, beyond the first layer. The exchange between the boundary and bilayer lipids takes at least 50 ns [38].

Recent NMR studies [16–19] have offered a different aspect. At or above the phase transition temperature, only one spectral component was observed for deuterated phospholipid in membranes containing cytochrome oxidase. This implies that the rate of exchange between the boundary and bilayer lipids exceeds 10^3 s^{-1}. Moreover, lipid chains were less ordered in the presence of the protein than in pure lipid membranes both below and above the phase transition. The disordering effect has been ascribed to irregular or rough surface of the protein with which the boundary lipid is in contact.

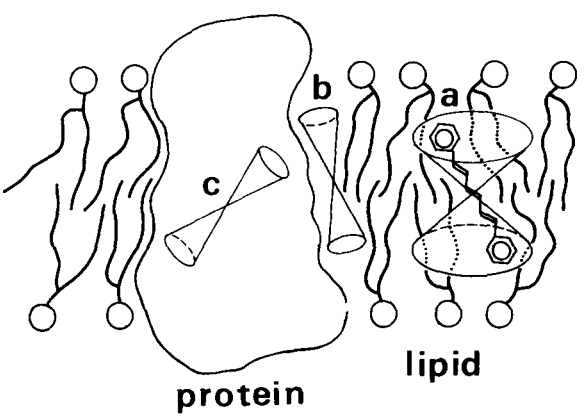

Fig. 5. Diagramatic representation of the wobbling motion of DPH in membrane. Cone a shows the approximate range of the nanosecond wobbling motion of DPH in bilayer part, which, in this figure, is assumed to be in the liquid-crystalline phase. A DPH molecule is depicted in this cone. Cones b and c show the motion on the surface of the protein. Lipid acyl chains probably exhibit similar, but not exactly the same, nanosecond wobbling motion. It is proposed that, during the time range of microseconds, DPH and lipid molecules move about freely among the different types of cones.

On the basis of our fluorescence data as well as the ESR and NMR results quoted above, we propose the following for the dynamics of lipid chains in membranes containing protein (Fig. 5). The essence is that there are two types of motion differing in their time range. In the nanosecond range, lipid chains in the bilayer region exhibit fast (D_w in the range of 0.02 to 0.2 ns^{-1}, depending on temperature) wobbling motion which is not much different from the motion in pure lipid. Wobbling motion of DPH, as represented by cone a in Fig. 5, closely reflects this chain motion. The order parameter for the bilayer lipid obtained by ESR relates to the cone angle *. According to Jost et al. [11], the ESR order parameter in the bilayer region of oxidase-containing membrane differs only slightly from that in pure lipid. At the surface of protein, on the other hand, chain motion is severely restricted in amplitude, though the average direction of a chain differs greatly depending on the position of the chain on the irregular surface of protein. Some of the chains may even be trapped in grooves on the surface. Motion of 'boundary' DPH is depicted as cones b and c in Fig. 5. The immobilization observed by ESR reflects this reduction in amplitude (θ_c) of the wobbling motion. The immobilization, however, is unlikely to be perfect even in the nanosecond range

* The order parameter corresponds to the square root of r_∞/r_0 [28,39], which in turn is related to the cone angle θ_c by $r_\infty/r_0 = \cos^2\theta_c(1 + \cos\theta_c)^2/4$ [1]. However, neither the cone angle, nor the ESR and NMR order parameters, obtained in suspensions necessarily represent order, if order implies parallelism among molecular orientations. These quantities relate to the angular range of wobbling motion of individual molecules as discussed in text. To estimate order in the above sense, one has to make measurement on oriented membranes. ESR measurements on oriented membranes in fact suggested that the orientation of lipid chains in the boundary region is random [11].

(see Fig. 3), and the chains must wobble rapidly in the narrow potential wells on the protein surface.

Here it is worth noting that, below the phase transition temperature, protein may even accelerate the wobbling motion (Fig. 3), though its amplitude remains small. Since cholesterol has a similar effect [7], one may generalize that a rigid, foreign molecule introduces, in its neighborhood, rapid wobbling motions even if the surrounding lipid is in the gel phase. The probable failure to accomodate neighboring chains with a close fit would allow more or less independent, and thus rapid, chain motions at the surface of the foreign molecule, in contrast to the cooperative chain wobbling in the bilayer region. Such unexpectedly rapid wobbling motion at low temperatures, however, may be peculiar to reconstituted membranes of relatively simple compositions. The wobbling motion of DPH in biological membranes is relatively slow, presumably because the various constituent molecules are arranged in a complementary manner that allows only concerted motions [29].

In the microsecond range, lipid molecules exchange their places as indicated by the NMR studies. On the protein surface, boundary lipid departs when thermal energy for the wobbling motion exceeds the depth of the potential well. These less frequent motions are not observed by fluorescence depolarization nor by conventional ESR spectroscopy, both of which are insensitive to microsecond reorientations. NMR, on the other hand, averages out these motions; the NMR order parameter would relate to the average over all types of cones, counting the difference in directions. Thus, protein disorders lipid chains when viewed by NMR.

The above is based on the behavior of DPH observed by nanosecond fluorescence depolarization. To what extent the wobbling motion of DPH simulates the motion of lipid chains in the boundary region remains open to question. However, we think that the nanosecond, small-angle wobbling of boundary lipid is a natural prerequisite to the slow exchange between the boundary lipid and the bilayer lipid (and between neighboring boundary lipid chains). A recent NMR study by Seelig et al. [40] has also shown that the presence of the Ca^{2+}-pump protein of sarcoplasmic reticulum leads to only a minor reduction of the rate of internal modes of phospholipid motions. The estimated values of the correlation time in DOPC bilayers (about 1 ns for the reorientation of phosphate group at 4°C, and 0.17 ns for the *cis* double bond at 21°C) are of the same order of magnitude as our φ in Table I.

It should also be pointed out that the difference in the cone angles between the boundary and bilayer DPH, as suggested in Fig. 5, is based largely on the ESR observations which indicated a distinct difference between the motional properties in the boundary and bilayer regions in the nanosecond time range. Though it is very likely that lipid chains or DPH pressed against the rigid, irregular protein wall will be more restricted in the wobbling range while they remain at the protein surface, the present experiments per se cannot eliminate an alternative interpretation, namely that the cone angles of both boundary and bilayer DPH were reduced in a similar manner as the protein/lipid ratio was increased. Then the only difference between the boundary and bilayer regions might be the variations in the direction of cone axes. A recent ESR study by Swanson et al. [41] has shown that, when cytochrome oxidase was dispersed in membranes of low protein/lipid ratio, the lipid fluidity in the vicinity of cytochrome oxidase as probed by a long-chain spin label covalently attached to the protein was only slightly lower than the fluidity in the bulk lipid. Whether the apparent discrepancy between their result and the previous ESR studies quoted above is ascribed to possible protein aggregation, as these authors suggest, or to, at least partially, the covalent linkage remains to be clarified.

Acknowledgements

We thank Dr. T. Shibata and Dr. K. Nagayama for clarifying discussions. Professor J. Seelig kindly made a preprint of his work available to us prior to publication. This work was supported by grants in aid from the Ministry of Education, Science and Culture of Japan, and by a research grant for 'Solar Energy Conversion-Photosynthesis' given by the Japan Science and Technology Agency.

References

1 Kinosita, K., Jr., Kawato, S. and Ikegami, A. (1977) Biophys. J. 20, 289–305

2 Chen, L.A., Dale, R.E., Roth, S. and Brand, L. (1977) J. Biol. Chem. 252, 2 163–2 169
3 Kawato, S., Kinosita, K., Jr. and Ikegami, A. (1977) Biochemistry 16, 2 319–2 324
4 Dale, R.E., Chen, L.A. and Brand, L. (1977) J. Biol. Chem. 252, 7 500–7 510
5 Lakowicz, J.R., Prendergast, F.G. and Hogen, D. (1979) Biochemistry 18, 508–519
6 Veatch, W.R. and Stryer, L. (1977) J. Mol. Biol. 117, 1 109–1 113
7 Kawato, S., Kinosita, K., Jr. and Ikegami, A. (1978) Biochemistry 17, 5 026–5 031
8 Sené, C., Genest, D., Obrénovitch, A., Wahl, P. and Monsigny, M. (1978) FEBS Lett. 88, 181–186
9 Hildenbrand, K. and Nicolau, C. (1979) Biochim. Biophys. Acta 553, 365–377
10 Jost, P.C., Griffith, O.H., Capaldi, R.A. and Vanderkooi, G. (1973a) Proc. Natl. Acad. Sci. U.S.A. 70, 480–484
11 Jost, P.C., Griffith, O.H., Capaldi, R.A. and Vanderkooi, G. (1937b) Biochim. Biophys. Acta 311, 141–152
12 Jost, P.C., Nadakavukaren, K.K. and Griffith, O.H. (1977) Biochemistry 16, 3 110–3 114
13 Warren, G.B., Houslay, M.D., Metcalfe, J.C. and Birdsall, N.J.M. (1975) Nature (London) 255, 684–687
14 Hesketh, T.R., Smith, G.A., Housley, M.D., McGill, K.A., Birdsall, N.J.M., Metcalfe, J.C. and Warren, G.B. (1976) Biochemistry 15, 4 145–4 151
15 Dahlquist, F.W., Muchmore, D.C., Davis, J.H. and Bloom, M. (1977) Proc. Natl. Acad. Sci. U.S.A. 74, 5 435–5 439
16 Seelig, A. and Seelig, J. (1978) Hoppe-Seyler's Z. Physiol. Chem. 359, 1 747–1 756
17 Oldfield, E., Gilmore, R., Glaser, M., Gutowsky, H.S., Hshung, J.C., Kang, S.Y., King, T.E., Meadows, M. and Rice, D. (1978) Proc. Natl. Acad. Sci. U.S.A. 75, 4 657–4 660
18 Kang, S.Y., Gutowsky, H.S., Hsung, J.C., Jacobs, R., King, T.E., Rice, D. and Oldfield, E. (1979) Biochemistry 18, 3 257–3 267
19 Rice, D.M., Hsung, J.C., King, T.E. and Oldfield, E. (1979) Biochemistry 18, 5 885–5 892
20 Yoshida, S., Orii, Y., Kawato, S. and Ikegami, A. (1979) J. Biochem. 86, 1 443–1 450
21 Kawato, S., Ikegami, A., Yoshida, S. and Orii, Y. (1980) Biochemistry 19, 1 598–1 603
22 Kawato, S., Yoshida, S., Orii, Y., Ikegami, A. and Kinosita, K.Jr. (1981) Biochim. Biophys. Acta 634, 85–92
23 Okunuki, K., Sekuzu, I., Takemori, S. and Yenetani, T. (1958) J. Biochem. 45, 847–854
24 Orii, Y. and Okunuki, K. (1965) J. Biochem. 58, 561–568
25 Kinosita, K., Jr., Mitaku, S., Ikegami, A., Ohbo, N. and Kunii, T.L. (1976) Jap. J. Appl. Phys. 15, 2 433–2 440
26 Shinitzky, M. and Barenholz, Y. (1974) J. Biol. Chem. 249, 2 652–2 657
27 Chapman, D., Williams, R.M. and Ladbrooke, B.D. (1967) Chem. Phys. Lipids 1, 445–475
28 Heyn, M.P. (1979) FEBS Lett. 108, 359–364
29 Kinosita, K., Jr., Kataoka, R., Kimura, Y., Gotoh, O. and Ikegami, A. (1981) Biochemistry, in the press
30 Shinitzky, M. and Barenholz, Y. (1978) Biochim. Biophys. Acta 515, 317–394
31 Förster, T. (1965) in Modern Quantum Chemistry (Sinanoglu, O., ed.), pp. 93–137, Academic Press, New York
32 Kawato, S., Sigel, E., Carafoli, E. and Cherry, J. (1980) J. Biol. Chem. 255, 5 508–5 510
33 Vanderkooi, G. (1974) Biochim. Biophys. Acta 344, 307–345
34 Fuller, S.D., Capaldi, R.A. and Henderson, R. (1979) J. Mol. Biol. 134, 305–327
35 Stubbs, G.W., Litman, B.J. and Barenholz, Y. (1976) Biochemistry 15, 2 766–2 772
36 Lentz, B.R., Barenholz, Y. and Thompson, T.E. (1976) Biochemistry 15, 4 521–4 528
37 Rigler, R. and Ehrenberg, M. (1973) Q. Rev. Biophys. 6, 139–199
38 Knowles, P.F., Watts, A. and Marsh, D. (1979) Biochemistry 18, 4 480–4 487
39 Jähnig, F. (1979) Proc. Natl. Acad. Sci. U.S.A. 76, 6 361–6 365
40 Seelig, J., Tamm, L., Hymel, L. and Fleischer, S. (1981) Biochemistry, in the press
41 Swanson, M.S., Quintanilha, A.T. and Thomas, D.D. (1980) J. Biol. Chem. 255, 7 494–7 502